

# Accepted Manuscript

Biotransformation of acyclovir by an enriched nitrifying culture

Yifeng Xu, Zhiguo Yuan, Bing-Jie Ni

PII: S0045-6535(16)31728-3

DOI: [10.1016/j.chemosphere.2016.12.014](https://doi.org/10.1016/j.chemosphere.2016.12.014)

Reference: CHEM 18469

To appear in: *ECSN*

Received Date: 15 September 2016

Revised Date: 2 December 2016

Accepted Date: 4 December 2016

Please cite this article as: Xu, Y., Yuan, Z., Ni, B.-J., Biotransformation of acyclovir by an enriched nitrifying culture, *Chemosphere* (2017), doi: 10.1016/j.chemosphere.2016.12.014.

This is a PDF file of an unedited manuscript that has been accepted for publication. As a service to our customers we are providing this early version of the manuscript. The manuscript will undergo copyediting, typesetting, and review of the resulting proof before it is published in its final form. Please note that during the production process errors may be discovered which could affect the content, and all legal disclaimers that apply to the journal pertain.



1                    **Biotransformation of Acyclovir by an Enriched Nitrifying Culture**

2  
3                    Yifeng Xu, Zhiguo Yuan, Bing-Jie Ni\*

4  
5                    Advanced Water Management Centre, The University of Queensland, St. Lucia, Brisbane, QLD

6                    4072, Australia

7  
8                    **\*Corresponding author:**

9                    Dr. Bing-Jie Ni

10                    Advanced Water Management Centre

11                    The University of Queensland

12                    Australia

13                    Phone: + 61 7 3346 3230

14                    Fax: +61 7 3365 4726

15                    E-mail: b.ni@uq.edu.au

16

17 **Abstract**

18 This work evaluates the biodegradation of the antiviral drug acyclovir by an enriched  
19 nitrifying culture during ammonia oxidation and without the addition of ammonium. The study  
20 on kinetics was accompanied with the structural elucidation of biotransformation products  
21 through batch biodegradation experiments at two different initial levels of acyclovir ( $15 \text{ mg L}^{-1}$   
22 and  $15 \text{ } \mu\text{g L}^{-1}$ ). The pseudo first order kinetic studies of acyclovir in the presence of ammonium  
23 indicated the higher degradation rates under higher ammonia oxidation rates than those constant  
24 degradation rates in the absence of ammonium. The positive correlation was found between  
25 acyclovir degradation rate and ammonia oxidation rate, confirming the cometabolism of  
26 acyclovir by the enriched nitrifying culture in the presence of ammonium. Formation of the  
27 product carboxy-acyclovir (P239) indicated the main biotransformation pathway was aerobic  
28 oxidation of the terminal hydroxyl group, which was independent on the metabolic type (i.e.  
29 cometabolism or metabolism). This enzyme-linked reaction might be catalyzed by  
30 monooxygenase from ammonia oxidizing bacteria or heterotrophs. The formation of carboxy-  
31 acyclovir was demonstrated to be irrelevant to the acyclovir concentrations applied, indicating  
32 the revealed biotransformation pathway might be the dominant removal pathway of acyclovir in  
33 wastewater treatment.

34

35 **Keywords:** Biotransformation; nitrification; cometabolism; ammonia oxidizing bacteria;  
36 acyclovir; wastewater treatment.

37

## 38 1. Introduction

39 In recent years, the increasing concerns have been focused on the emerging pharmaceuticals  
40 in aquatic environment due to their potential hazardous effects on living organisms (Daughton  
41 and Ternes, 1999; Kümmerer, 2009; Sirés and Brillas, 2012). Large amounts of pharmaceuticals  
42 were used by human beings or manufactured for veterinary drugs, leading to their widespread  
43 occurrence in the wastewater, surface water and ground water (Luo et al., 2014). Wastewater  
44 treatment plant (WWTP) was an important pathway for pharmaceuticals entering into the  
45 environment (Kosma et al., 2010; Tijani et al., 2013). Inefficient removal efficiencies of these  
46 compounds were observed during treatment processes because WWTPs were mainly designed  
47 for bulk nutrient removal (Joss et al., 2006; Kosma et al., 2014; Ternes, 1998).

48 Nitrification process was observed to be able to enhance the removal of pharmaceuticals  
49 (Batt et al., 2006; Fernandez-Fontaina et al., 2012). The involved ammonia oxidizing bacteria  
50 (AOB) were probably responsible for cometabolic biodegradation of pharmaceuticals due to its  
51 non-specific enzyme ammonia monooxygenase (AMO), which was confirmed to degrade a  
52 broad range of organic substrates including aliphatic and aromatic compounds (Keener and Arp,  
53 1994; Lauchnor and Semprini, 2013; Rasche et al., 1990; Skotnicka-Pitak et al., 2009).  
54 Furthermore, biotransformation products formed during treatment processes may be more  
55 persistent and could probably contribute to the overall toxicity (Miao and Metcalfe, 2003; Pérez  
56 et al., 2006; Quintana et al., 2005; Ternes et al., 2007). Therefore, the biotransformation products  
57 should also be considered in order to get a comprehensive understanding of the behavior and fate  
58 of pharmaceuticals in the environment and engineered systems.

59 As an important antiviral drug, acyclovir has been consumed largely especially for influenza  
60 epidemics. Due to their potential ecosystem alterations and the development of viral resistances,

61 antiviral drugs have recently attracted the interest of research. For example, a substantial removal  
62 (98%) of acyclovir was found in the wastewater treatment with the concentration decreasing  
63 from 1780 ng L<sup>-1</sup> to 27 ng L<sup>-1</sup> (Prasse et al., 2010). Although lab-scale biodegradation of  
64 acyclovir was previously studied by the activated sludge from the nitrification zone of a real  
65 wastewater treatment plant (Prasse et al., 2011), the effect of metabolic conditions on the  
66 formation of biotransformation products and the specific contributions of AOB and heterotrophs  
67 to acyclovir removal has not been clearly defined so far.

68 This study aims to investigate the biodegradation kinetics, products and pathways of  
69 acyclovir by an enriched nitrifying culture through batch biodegradation experiments under  
70 different metabolic conditions, i.e., with and without the addition of growth substrate,  
71 ammonium. The kinetic analysis was accompanied with the structural elucidation of  
72 biotransformation products. The initial acyclovir concentration at 15 mg L<sup>-1</sup> and 15 µg L<sup>-1</sup> were  
73 applied to verify if the biotransformation products and pathways formed under high  
74 concentration would occur at environmentally relevant levels.

75

## 76 **2. Materials and Methods**

77

### 78 **2.1 Chemicals**

79 Acyclovir (>98%) was purchased from Thermo Fisher, Australia. Carboxy-acyclovir was  
80 provided by Toronto Research Chemicals. Isotope labeled compound acyclovir-d4 was obtained  
81 from Santa Cruz Biotechnology. HPLC grade organic solvents (methanol, acetonitrile, hexane  
82 and acetone) were supplied by Sigma-Aldrich, Australia. The individual standard stock solution  
83 of acyclovir was prepared on a weight basis in methanol at 1 mg mL<sup>-1</sup> and stored at -20 °C. The

84 calibration curve was obtained by diluting the stock solution appropriately in methanol/water  
85 (25:75, v/v). Acyclovir feed solution used in the batch experiments was prepared in Milli-Q  
86 water (Millipore, Inc.) at initial concentration of  $1 \text{ g L}^{-1}$ .

87

## 88 **2.2 Enriched nitrifying culture**

89 An 8-L lab-scale sequencing batch reactor (SBR) was inoculated with the activated sludge  
90 from a domestic wastewater treatment plant in Brisbane, Australia. It was operated with the aim  
91 for the enrichment of nitrifying culture (containing AOB and nitrite oxidizing bacteria (NOB) to  
92 perform full nitrification) in cycles of 6 h. For each cycle, it consisted of aerobic feeding (260  
93 min), aeration (30 min), waste (1 min), settling (60 min) and decanting (9 min). 2 L synthetic  
94 wastewater consisting of  $1 \text{ g L}^{-1} \text{ NH}_4^+\text{-N}$  was fed into the reactor during each feeding period,  
95 resulting in a hydraulic retention time (HRT) of 24 h. The solid retention time (SRT) was  
96 controlled at around 15 d. Dissolved oxygen (DO) was controlled between  $2.5\text{-}3.0 \text{ mg L}^{-1}$  using  
97 programmed logic controllers (PLC) and pH was maintained at the range of 7.5-8.0.

98 The synthetic wastewater for the enriching the nitrifying culture contained per liter (Kuai  
99 and Verstraete, 1998): 5.63 g of  $\text{NH}_4\text{HCO}_3$  ( $1 \text{ g NH}_4^+\text{-N}$ ), 5.99 g of  $\text{NaHCO}_3$ , 0.064 g of each of  
100  $\text{KH}_2\text{PO}_4$  and  $\text{K}_2\text{HPO}_4$  and 2 mL of a trace element solution. The trace element stock solution  
101 contained:  $1.25 \text{ g L}^{-1}$  EDTA,  $0.55 \text{ g L}^{-1}$   $\text{ZnSO}_4\cdot 7\text{H}_2\text{O}$ ,  $0.40 \text{ g L}^{-1}$   $\text{CoCl}_2\cdot 6\text{H}_2\text{O}$ ,  $1.275 \text{ g L}^{-1}$   
102  $\text{MnCl}_2\cdot 4\text{H}_2\text{O}$ ,  $0.40 \text{ g L}^{-1}$   $\text{CuSO}_4\cdot 5\text{H}_2\text{O}$ ,  $0.05 \text{ g L}^{-1}$   $\text{Na}_2\text{MoO}_4\cdot 2\text{H}_2\text{O}$ ,  $1.375 \text{ g L}^{-1}$   $\text{CaCl}_2\cdot 2\text{H}_2\text{O}$ ,  $1.25$   
103  $\text{g L}^{-1}$   $\text{FeCl}_3\cdot 6\text{H}_2\text{O}$  and  $44.4 \text{ g L}^{-1}$   $\text{MgSO}_4\cdot 7\text{H}_2\text{O}$ .

104 The biodegradation experiments in this study were conducted after more than 1 year of  
105 stable reactor operation with the AOB and NOB population accounting for over 80% of the  
106 microbial community with almost 100% conversion of  $\text{NH}_4^+$  to  $\text{NO}_3^-$ . The mixed liquor volatile

107 suspended solids (MLVSS) concentration was stable at  $1437.6 \pm 112.9 \text{ mg L}^{-1}$  (mean and  
108 standard errors, respectively,  $n=10$ ). According to the microbial community analysis with  
109 fluorescence in situ hybridization (FISH) (Law et al., 2011), ammonia-oxidizing *beta-*  
110 *proteobacteria* accounted for  $46 \pm 6\%$  ( $n=20$ ) of the bacterial populations and the *Nitrospira*  
111 genera (nitrite oxidizers) constituted  $38 \pm 5\%$  ( $n=20$ ) of the bacterial populations.

112

### 113 **2.3 Batch experiments**

114 All batch experiments were conducted in 4 L beakers coupled with PLC controllers.  
115 Enriched nitrifying biomass was withdrawn from the SBR during aeration phase when  
116 ammonium was almost depleted. The biomass was added into the beaker to obtain the MLVSS  
117 concentration of approximately  $1000 \text{ mg L}^{-1}$  at the beginning of the batch tests. All the batch  
118 experiments were divided into two series according to the initial acyclovir concentration. High  
119 concentration ( $15 \text{ mg L}^{-1}$ ) was selected to identify any possible biotransformation products and  
120 elucidate the biotransformation pathways while low concentration ( $15 \mu\text{g L}^{-1}$ ) was used to study  
121 its degradation profile and verify the biotransformation products under environmentally relevant  
122 concentration. For each concentration level, different sets of experiments were performed (in  
123 duplicates for each experiment) (Table 1). EXP1 was conducted to assess biodegradation of  
124 acyclovir in the presence of ammonium. The constant ammonium concentration ( $50 \text{ mg L}^{-1}$ ) was  
125 provided by automatically adding a mixture of ammonium bicarbonate and sodium bicarbonate,  
126 which was controlled by PLC as a pH adjustment process. The adding volume was controlled to  
127 be minor, which would not change the total volume significantly. EXP2 was performed in the  
128 absence of ammonium during the overall time course. EXP3 was carried out with the initial  
129 addition of allylthiourea (ATU), which could inhibit ammonia oxidation probably by chelating

130 the copper of AMO active site (Ginestet et al., 1998). The control experiments, EXP4 and EXP5,  
131 were used to assess the contribution of abiotic degradation and hydrolytic degradation to  
132 acyclovir losses using  $\text{NaN}_3$  and pure water (without biomass), respectively.  $\text{NaN}_3$  was a  
133 chemical inhibitor used for the inactivation of microbial activities (Rattier et al., 2014). Aerobic  
134 conditions were achieved with controlled air supply to obtain DO concentration of  $2.5\text{-}3.0\text{ mg L}^{-1}$ .  
135 The pH was maintained in the range of 7.5-8.0 during the time course in all tests. Mixed liquor  
136 samples were taken periodically and immediately frozen until analysis.

137

#### 138 **2.4 Sample preparation and chemical analysis**

139 For experiments at initial acyclovir concentration of  $15\text{ mg L}^{-1}$ , samples were centrifuged at  
140  $12000\text{ g}$  for 5 min without filtration to obtain 1 mL supernatant for further direct structural  
141 elucidation of the biotransformation products and quantification. For experiments at initial  
142 acyclovir concentration of  $15\text{ }\mu\text{g L}^{-1}$ , the samples were concentrated through solid phase  
143 extraction (SPE) with vacuum manifold (J. T. Baker, The Netherlands) with the recovery for  
144 acyclovir of  $87.2 \pm 6.4\%$  ( $n=3$ ,  $10\text{ }\mu\text{g L}^{-1}$  added). 50 mL samples were first centrifuged at 14000  
145 rpm for 5 min. The supernatant was flowing through Oasis HLB cartridges (6 mL, 200 mg,  
146 Waters, USA) at a rate of  $5\text{ mL min}^{-1}$  after conditioned with 10 mL methanol and 10 mL Milli-Q  
147 water. Then cartridges were dried under vacuum for 30 min before they were eluted with 10 mL  
148 methanol and 10 mL of hexane/acetone (50:50, v/v). The extracted elutes were evaporated to  
149 dryness under gentle nitrogen stream. The residue was reconstituted in 250  $\mu\text{L}$  methanol and 750  
150  $\mu\text{L}$  Milli-Q water with 20  $\mu\text{L}$  acyclovir-d4 (internal standard) added before further analysis.

151 The samples were analyzed by the ultra-fast liquid chromatography (UFLC) (Shimadzu,  
152 Japan) coupled with a 4000 QTRAP hybrid triple quadruple-linear ion trap mass spectrometer



153 (QqLIT-MS) equipped with a Turbo Ion Spray source (Applied Biosystems-Sciex, USA).  
154 Chromatographic separation was carried out with the injection volume of 20  $\mu\text{L}$  using an Alltima  
155 C18 column (Alltech Associates Inc., USA) at 40  $^{\circ}\text{C}$ . The mobile phase contained (A)  $\text{H}_2\text{O}$  and  
156 (B)  $\text{CH}_3\text{CN}$  at a flow rate of 1  $\text{mL min}^{-1}$ . The gradient of (B) was conducted as follows: it was  
157 linearly increased to 5% B after 0.5 min, further increased to 20% B for 12.5 min, increased to  
158 50% B within 5 min, increased to 100% B for 2 min, kept constant for 4 min and finally was  
159 decreased to 5% B for 1 min. The total running time including the conditioning of the column to  
160 the initial conditions was 27 min. Positive electrospray ionization (ESI+) mode was applied with  
161 the corresponding parameters: drying gas temperature of 500  $^{\circ}\text{C}$ , drying gas 50 psi, curtain gas  
162 30 psi, spraying gas 50 psi. Tentative structures of biotransformation products were identified  
163 using the full scan mode at a declustering potential of 80 V and mass range of 50-300 amu  
164 followed by the product ion scan mode ( $\text{MS}^2$ ) and sequential fragmentation using the ion trap.  
165 Concentrations of acyclovir and its biotransformation product were analyzed in the multiple  
166 reaction monitoring (MRM) mode with two transition ions for confirmation and quantification,  
167 respectively. The samples from the experiments at initial 15  $\text{mg L}^{-1}$  acyclovir need to be diluted  
168 100 times in methanol/Milli-Q water (25:75, v/v) prior to quantification. More detailed  
169 information could be obtained in Table S1 in the supporting information (SI).

170 Ammonium ( $\text{NH}_4^+\text{-N}$ ) concentrations controlled in the batch biodegradation experiments  
171 were measured with a Lachat QuikChem8000 Flow Injection Analyzer (Lachat Instrument,  
172 Milwaukee) and were shown in Figure S1 in SI. Nitrite was not accumulated significantly with  
173 the concentration lower than 1  $\text{mg L}^{-1}$  for the experimental period and same nitrate concentration  
174 was observed as the SBR effluent (up to 1000  $\text{mg L}^{-1}$ ).

175

### 176 3. Results

177

#### 178 3.1 Control experiments

179 The sorption ability of acyclovir onto the biomass was considered negligible due to the low  
180 value of octanol-water partition coefficient ( $\text{Log } K_{ow}$ , -1.59) (Kasim et al., 2004), which could  
181 also be observed from the control experimental results in this study. Regardless of the initial  
182 concentration of acyclovir, both abiotic control (EXP4) and hydrolytic control (EXP5)  
183 experiments demonstrated the stability of acyclovir over the time course without any  
184 transformation products (Figure S2). Sorption and hydrolysis would not contribute to acyclovir  
185 removal. Given that the reactors were covered with aluminum foil from photodegradation,  
186 biodegradation by nitrifying biomass was the major pathway for acyclovir removal in all the  
187 experiments.

188

#### 189 3.2 Acyclovir biodegradation in the presence of ammonium

190 The removal efficiency, transformation efficiency and degradation constant of acyclovir in  
191 all the biodegradation experiments were summarized in Table 2. Figure 1 shows the results from  
192 the biodegradation experiments in the presence of ammonium. The decrease of acyclovir and  
193 formation of the product were plotted using their respective concentrations normalized to the  
194 initial acyclovir concentration. At initial concentration of  $15 \text{ mg L}^{-1}$ , acyclovir underwent a  
195 gradual decrease with approximately 65.1% removal at the end of experiments (Figure 1A).  
196 After careful screening in the full scan chromatogram followed by spectrum analysis based on  
197 nitrogen rule and the existence of the peak  $[m+\text{Na}]$ , etc, one major biotransformation product  
198 P239 was found at retention time of 4.88 min (data not shown) with nominal mass of 239. Its

199 structural elucidation was carried out in the following section 3.5. With the available reference  
200 standard (carboxy-acyclovir), it was increased gradually from the beginning of the experiments  
201 to  $6.95 \text{ mg L}^{-1}$  (58.6% of conversion rate) at 240 h.

202 At initial  $15 \text{ } \mu\text{g L}^{-1}$  concentration, the removal efficiency for acyclovir (88.2%) was higher  
203 than that obtained at higher initial level (65.1%) (Figure 1B). The same major product P239 was  
204 continuously increased to  $5.74 \text{ } \mu\text{g L}^{-1}$ . Only 33.0% of the removed parent compound was  
205 transformed to P239 while the remaining might be transformed to other minor products or  
206 mineralized.

207 For both initial concentration levels, acyclovir biodegradation followed the pseudo first  
208 order degradation kinetics (Figure S3). Same as their concentration profiles, acyclovir also  
209 showed the higher degradation constant ( $0.0071 \text{ L g}_{\text{VSS}}^{-1} \text{ h}^{-1}$ ) at initial  $15 \text{ } \mu\text{g L}^{-1}$  concentration  
210 than  $0.0034 \text{ L g}_{\text{VSS}}^{-1} \text{ h}^{-1}$  at  $15 \text{ mg L}^{-1}$  concentration. These degradation constants were lower than  
211 the reported value ( $4.9 \text{ L g}_{\text{SS}}^{-1} \text{ d}^{-1}$ ) (Prasse et al., 2011), probably due to unaccustomed sludge to  
212 acyclovir. Long-term adaption to pharmaceuticals would enhance the degradation ability of the  
213 activated sludge (Pomiès et al., 2015). The decreasing ammonia oxidation rate observed during  
214 the experimental period (Figure 2A) might be due to the inhibition of acyclovir or its  
215 transformation product (Radniechi et al., 2008; Sathyamoorthy et al., 2013), which could lead to  
216 decreasing rates of both substrates. NOB has been proved to be not associated with  
217 pharmaceutical (e.g., atenolol) degradation in previous work, with AMO as the main responsible  
218 of the cometabolism (Fernandez-Fontaina et al., 2012; Sathyamoorthy et al., 2013; Xu et al.,  
219 2016). Regardless of initial acyclovir concentration, the positive relationship between acyclovir  
220 degradation rate and ammonia oxidation rate suggested the cometabolic biodegradation of  
221 acyclovir by AOB in the presence of ammonium (Figure 2B). The cometabolism also applies to

222 higher concentration of non-growth substrate although it was in the range of the growth substrate  
223 concentration (Quintana et al., 2005).

224

### 225 **3.3 Acyclovir biodegradation in the absence of ammonium**

226 Without the presence of growth substrate, acyclovir was removed by enriched nitrifying  
227 biomass up to 40.9% with the final concentration being  $8.5 \text{ mg L}^{-1}$  for the higher initial acyclovir  
228 concentration experiments (Figure 3A). Simultaneously, the product P239 showed a rapid  
229 growing profile compared with the results from experiments with ammonia oxidation. Its  
230 concentration was quantified as  $8.7 \text{ mg L}^{-1}$  at 240 h. Nearly constant mass balance during the  
231 time course indicated that almost all the acyclovir removed in the absence of ammonium was  
232 transformed to P239. Furthermore, the mass balance did not show a decreasing trend even after  
233 15 d. Thus, P239 might be the only biotransformation product.

234 For the low initial acyclovir experiments, the removal rate of acyclovir only reached up to  
235 47.8% without ammonia oxidation, which was significantly lower than that observed in the  
236 presence of ammonium (88.2%) (Figure 3B). Regardless of the initial acyclovir concentration,  
237 the cometabolism in the obligatory presence of growth substrate played a positive role in  
238 degrading acyclovir than the metabolic degradation without ammonia oxidation. The formation  
239 of P239 showed a slower increasing trend compared to that observed in the high initial acyclovir  
240 concentration experiments.

241 The linear regression on the concentration profiles of acyclovir in Figures S4A and B  
242 demonstrated the constant degradation rate of acyclovir in the biodegradation experiments  
243 without ammonia oxidation. Acyclovir degradation rates during the higher initial concentration  
244 and lower initial concentration experiments were  $0.027 \text{ mg g}_{\text{VSS}}^{-1} \text{ h}^{-1}$  and  $0.043 \text{ } \mu\text{g g}_{\text{VSS}}^{-1} \text{ h}^{-1}$ ,

245 respectively, which were lower than their corresponding degradation rates (0.051, 0.046, 0.042,  
246 0.038, 0.034, 0.031, 0.028 mg gvss<sup>-1</sup> h<sup>-1</sup> and 0.18, 0.15, 0.12, 0.090, 0.071, 0.056, 0.044 µg gvss<sup>-1</sup>  
247 h<sup>-1</sup> at time 0, 24, 48, 72, 96, 120, 144 h) under higher ammonia oxidation rates in the experiments  
248 in the presence of ammonium, further confirmed the important role of cometabolic  
249 biodegradation by AOB for acyclovir removal.

250

### 251 **3.4 Acyclovir biodegradation with ATU inhibition**

252 ATU was added at the beginning of the experiments in order to inhibit the nitrifying  
253 activities of AOB, thus likely leading to the exclusive degradation of acyclovir by heterotrophs.  
254 As no external organic source was provided in the experiments, acyclovir degradation might  
255 attribute to heterotrophic metabolic activity. Figure 4A illustrates that acyclovir experienced a  
256 slow gradual decrease with a removal rate of 36.2% over the experimental period at the higher  
257 initial concentration, which was slightly lower than 40.9% obtained in the absence of  
258 ammonium. P239 was still the only product formed with the concentration increasing to 6.4 mg  
259 L<sup>-1</sup> when nitrifying activities were inhibited. Practically 94.1% of the consumed acyclovir was  
260 transformed to P239 and the mass balance leveled off for the overall time course. Therefore, no  
261 other major products might be formed by heterotrophs.

262 As shown in Figure 4B, acyclovir at initial 15 µg L<sup>-1</sup> also declined gradually with a removal  
263 efficiency of 50.3% accompanied by the continuous increase of its product P239 (4.9 µg L<sup>-1</sup> at  
264 240 h). The mass balance analysis also indicated the constant mass during the experimental  
265 period with only one product P239 formed.

266 The linear regression in Figures S4C and D showed acyclovir degradation constants for  
267 experiments at the higher initial concentration and the lower initial concentration were calculated

268 as  $0.02 \text{ mg g}_{\text{VSS}}^{-1} \text{ h}^{-1}$  and  $0.018 \text{ } \mu\text{g g}_{\text{VSS}}^{-1} \text{ h}^{-1}$ , respectively. Compared to the values obtained in  
269 the absence of ammonium, heterotrophs played a major contribution to acyclovir degradation  
270 under the condition without ammonia oxidation by AOB. The role of AOB and heterotrophs has  
271 been investigated in previous studies on pharmaceutical biodegradation (Khunjar et al., 2011;  
272 Tran et al., 2013). The fact that the same biotransformation products for 17 $\beta$ -ethinylestradiol  
273 were formed by AOB or heterotrophs (Khunjar et al., 2011) was consistent to the observations in  
274 this study. The results confirmed that P239 was the major biotransformation product of acyclovir  
275 by the enriched culture independent on its initial concentration.

276

### 277 **3.5 Structural elucidation of biotransformation product**

278 The full scan chromatogram of the samples indicated the formation of the product P239  
279 during all biodegradation experiments. Its structure was then identified through the analysis and  
280 comparison of the product ion ( $\text{MS}^2$ ) spectrum of the biodegradation samples with that of the  
281 available standard carboxy-acyclovir. Figure 5 showed the  $\text{MS}^2$  spectrum of the molecular ion  
282  $m/z$  240, which was the protonated P239. The most abundant fragment ions were  $m/z$  152 and  
283 135. The molecular ion  $m/z$  240 underwent the loss of 88 Da to produce the fragment ion  $m/z$  152.  
284 Further fragmentation of  $m/z$  152 led to a loss of  $\text{NH}_3$  molecule to form  $m/z$  135. The similar  
285 fragmentation pattern was previously reported in the literature (Prasse et al., 2011). Another  
286 minor fragmentation pathway was to form  $m/z$  122 with a loss of 44 Da from  $m/z$  164, following  
287 the loss of 76 Da from molecular ion  $m/z$  240. Collision induced dissociation of the molecular  
288 ion  $m/z$  240 could lead to the third route to obtain the fragment ion  $m/z$  61, via the formation of  
289 the fragment ion 89. There were no further fragmentation pathways from the lowest  $m/z$  61. The  
290 same fragment ions and fragment pattern observed in the standard solution further confirmed that

291 P239 could be assigned to 9-carboxymethoxymethylguanine (carboxy-acyclovir) (Figure S5).

292 The same fragment ions  $m/z$  152 and 135 were also formed in the MS<sup>2</sup> spectrums of the  
293 parent compound acyclovir, except  $m/z$  164 and 122, which were also reported in previous  
294 literature (Prasse et al., 2011). The only difference between acyclovir and P239 was the third  
295 pathway forming  $m/z$  75 and  $m/z$  89, respectively (Figure S6), which was attributed to the  
296 oxidation of the hydroxyl group to the carboxy group. This also supported the structural  
297 identification of P239 in this work.

298

#### 299 4. Discussion

300 In this work, the biodegradation of the antiviral drug acyclovir by an enriched nitrifying  
301 culture was investigated during ammonia oxidation and without the addition of ammonium.  
302 Acyclovir degradation rates based on pseudo first order kinetics under higher ammonia oxidation  
303 rate in the presence of ammonium were higher than those constant values in the absence of  
304 ammonium. The positive correlation observed between acyclovir degradation rate and ammonia  
305 oxidation rate further confirmed the cometabolism of acyclovir by the enriched nitrifying culture  
306 in the presence of ammonium, which was also supported from the similar relationship for 17 $\alpha$ -  
307 ethinylestradiol (Yi and Harper, 2007).

308 Based on the identified product, the main biotransformation pathway was proposed for  
309 acyclovir degradation: from acyclovir to carboxy-acyclovir (P239). This reaction was attributed  
310 to the oxidation of the terminal hydroxyl group to the carboxy group, which was typically  
311 catalyzed by AMO from AOB or ammonia oxidizing archaea (AOA) for most pharmaceuticals  
312 including other antiviral drugs (abacavir, emtricitabine, ganciclovir, lamivudine and zidovudine),  
313 amide-containing compounds (e.g. propachlor) and tertiary amines such as mianserin (Funke et

314 al., 2016; Helbling et al., 2010; Men et al., 2016). Although it was also observed in mammalian  
315 metabolism of acyclovir (Prasse et al., 2011), the enzyme-induced alcohol oxidation has not been  
316 investigated solely for heterotrophs previously. However, the formation of carboxy-acyclovir in  
317 experiments with ATU addition in this work indicated that the monooxygenase from  
318 heterotrophs could also catalyze the alcohol oxidation of such compound. Although other  
319 possibly formed products were not identified in the presence of ammonium, the same  
320 biotransformation product carboxy-acyclovir found with ammonia oxidation and with  
321 nitrification inhibited in this study was different from previous report on iopromide, where  
322 dehydroxylated and carboxylated products were formed, respectively (Batt et al., 2006). It was  
323 proposed that oxidation of acyclovir to carboxy-acyclovir might be catalyzed by monooxygenase  
324 from either AOB or heterotrophs (Men et al., 2016).

325 It was also noted that the formation of carboxy-acyclovir was independent on the metabolic  
326 type, i.e. regardless of the presence of ammonia oxidation by AOB. This was contradictory to the  
327 observation that the generation of 4-chlorobenzoic acid was related to the metabolic type and  
328 only produced by microbial hydrolysis of the amide bond of bezafibrate under cometabolism  
329 (Quintana et al., 2005). Comparing with acyclovir, the human metabolite carboxy-ibuprofen was  
330 not found in biodegradation of ibuprofen following alcohol oxidation (Quintana et al., 2005).  
331 The possible reason could be related to the specific structures of the studied pharmaceuticals.  
332 The guanine group of acyclovir showed no significant changes during biodegradation with the  
333 primary hydroxyl being the only vulnerable group. However, whether acyclovir could be  
334 biotransformed to other products is not confirmed in the product identification in this study  
335 although the mass balance analysis in the presence of ammonium demonstrated the possible  
336 formation of other products. Further work would be required to confirm the thorough



337 biotransformation pathway of acyclovir.

338 The biotransformation pathway to carboxy-acyclovir by enriched nitrifying cultures was  
339 independent of the initial concentration of acyclovir, i.e.  $15 \mu\text{g L}^{-1}$  or  $15 \text{mg L}^{-1}$ . This was in  
340 consistent with the previous study on trimethoprim by nitrifying activated sludge (Eichhorn et  
341 al., 2005). Two metabolites were formed and the degradation route was independent on the  
342 initial concentration of trimethoprim ( $20 \text{mg L}^{-1}$  or  $20 \mu\text{g L}^{-1}$ ). However, biodegradation of  
343 trimethoprim was also investigated by nitrifying activated sludge in another recent study (Jewell  
344 et al., 2016), resulting in different biotransformation products under different spiked  
345 concentration of trimethoprim ( $500 \mu\text{g L}^{-1}$  or  $5 \mu\text{g L}^{-1}$ ). From the mass balance analysis, carboxy-  
346 acyclovir seems to be the only product by heterotrophs either in higher initial concentration or  
347 lower initial concentration of acyclovir. There might be other minor biotransformation products  
348 formed through cometabolism by enriched nitrifying cultures as carboxy-acyclovir had a low  
349 final percentage and the total mass showed a decreasing trend, which was vastly different from  
350 those under other conditions (in the absence of ammonium and with addition of ATU), which  
351 could not be confirmed yet currently and required future efforts.

352

## 353 5. Conclusion

354 Biodegradation of acyclovir by an enriched nitrifying culture was investigated during  
355 ammonia oxidation and without the presence of ammonium at different initial concentrations of  
356 acyclovir in this study. The key conclusions are:

- 357 • Biodegradation of acyclovir was positively related to the ammonia oxidation rate, confirmed  
358 the key role of cometabolism by AOB in acyclovir removal.
- 359 • Carboxy-acyclovir was produced from acyclovir regardless of the presence of ammonium

360 and thus unaffected by metabolic type.

361 • The same biotransformation pathway from acyclovir to carboxy-acyclovir was observed at  
362 different initial concentrations of acyclovir.

363 • Alcohol oxidation was the biotransformation reaction catalyzed by non-specific enzyme  
364 monooxygenase, probably either from AOB or heterotrophs.

365

### 366 **Acknowledgement**

367 This study was supported by the Australian Research Council (ARC) through Discovery  
368 Early Career Researcher Award DE130100451. Bing-Jie Ni acknowledges the support of ARC  
369 Discovery Project DP130103147 and The University of Queensland Foundation Research  
370 Excellence Award.

371

### 372 **Reference**

373 Batt, A.L., Kim, S., Aga, D.S., 2006. Enhanced biodegradation of iopromide and trimethoprim in  
374 nitrifying activated sludge. *Environ. Sci. Technol.* 40, 7367-7373.

375 Daughton, C.G., Ternes, T.A., 1999. Pharmaceuticals and personal care products in the  
376 environment: Agents of subtle change? *Environ. Health Perspect.* 107, 907-938.

377 Eichhorn, P., Ferguson, P.L., Pérez, S., Aga, D.S., 2005. Application of ion trap-MS with H/D  
378 exchange and QqTOF-MS in the identification of microbial degradates of trimethoprim in  
379 nitrifying activated sludge. *Anal. Chem.* 77, 4176-4184.

380 Fernandez-Fontaina, E., Omil, F., Lema, J.M., Carballa, M., 2012. Influence of nitrifying  
381 conditions on the biodegradation and sorption of emerging micropollutants. *Water Res.* 46,  
382 5434-5444.

- 383 Funke, J., Prasse, C., Ternes, T.A., 2016. Identification of transformation products of antiviral  
384 drugs formed during biological wastewater treatment and their occurrence in the urban water  
385 cycle. *Water Res.* 98, 75-83.
- 386 Ginestet, P., Audic, J.M., Urbain, V., Block, J.C., 1998. Estimation of nitrifying bacterial  
387 activities by measuring oxygen uptake in the presence of the metabolic inhibitors  
388 allylthiourea and azide. *Appl. Environ. Microbiol.* 64, 2266-2268.
- 389 Helbling, D.E., Hollender, J., Kohler, H.-P.E., Fenner, K., 2010. Structure-based interpretation of  
390 biotransformation pathways of amide-containing compounds in sludge-seeded bioreactors.  
391 *Environ. Sci. Technol.* 44, 6628-6635.
- 392 Jewell, K.S., Castronovo, S., Wick, A., Falås, P., Joss, A., Ternes, T.A., 2016. New insights into  
393 the transformation of trimethoprim during biological wastewater treatment. *Water Res.* 88,  
394 550-557.
- 395 Joss, A., Zabczynski, S., Göbel, A., Hoffmann, B., Löffler, D., Mc Ardell, C.S., Ternes, T.A.,  
396 Thomsen, A., Siegrist, H., 2006. Biological degradation of pharmaceuticals in municipal  
397 wastewater treatment: Proposing a classification scheme. *Water Res.* 40, 1686-1696.
- 398 Kasim, N.A., Whitehouse, M., Ramachandran, C., Bermejo, M., Lennernäs, H., Hussain, A.S.,  
399 Junginger, H.E., Stavchansky, S.A., Midha, K.K., Shah, V.P., Amidon, G.L., 2004.  
400 Molecular properties of WHO essential drugs and provisional biopharmaceutical  
401 classification. *Mol. Pharmaceutics* 1, 85-96.
- 402 Keener, W.K., Arp, D.J., 1994. Transformations of aromatic compounds by *Nitrosomonas*  
403 *europaea*. *Appl. Environ. Microbiol.* 60, 1914-1920.
- 404 Khunjar, W.O., Mackintosh, S.A., Skotnicka-Pitak, J., Baik, S., Aga, D.S., Love, N.G., 2011.  
405 Elucidating the relative roles of ammonia oxidizing and heterotrophic bacteria during the

- 406 biotransformation of 17 $\alpha$ -ethinylestradiol and trimethoprim. Environ. Sci. Technol. 45,  
407 3605-3612.
- 408 Kosma, C.I., Lambropoulou, D.A., Albanis, T.A., 2010. Occurrence and removal of PPCPs in  
409 municipal and hospital wastewaters in Greece. J. Hazard. Mater. 179, 804-817.
- 410 Kosma, C.I., Lambropoulou, D.A., Albanis, T.A., 2014. Investigation of PPCPs in wastewater  
411 treatment plants in Greece: Occurrence, removal and environmental risk assessment. Sci.  
412 Total Environ. 466–467, 421-438.
- 413 Kuai, L., Verstraete, W., 1998. Ammonium removal by the oxygen-limited autotrophic  
414 nitrification- denitrification system. Appl. Environ. Microbiol. 64, 4500-4506.
- 415 Kümmerer, K., 2009. The presence of pharmaceuticals in the environment due to human use –  
416 present knowledge and future challenges. J. Environ. Manage. 90, 2354-2366.
- 417 Lauchnor, E.G., Semprini, L., 2013. Inhibition of phenol on the rates of ammonia oxidation by  
418 *Nitrosomonas europaea* grown under batch, continuous fed, and biofilm conditions. Water  
419 Res. 47, 4692-4700.
- 420 Law, Y., Lant, P. Yuan, Z., 2011. The effect of pH on N<sub>2</sub>O production under aerobic conditions  
421 in a partial nitrification system. Water Res. 45, 5934-5944.
- 422 Luo, Y., Guo, W., Ngo, H.H., Nghiem, L.D., Hai, F.I., Zhang, J., Liang, S., Wang, X.C., 2014. A  
423 review on the occurrence of micropollutants in the aquatic environment and their fate and  
424 removal during wastewater treatment. Sci. Total Environ. 473-474, 619-641.
- 425 Men, Y., Han, P., Helbling, D.E., Jehmlich, N., Herbold, C., Gulde, R., Onnis-Hayden, A., Gu,  
426 A.Z., Johnson, D.R., Wagner, M., Fenner, K., 2016. Biotransformation of Two  
427 Pharmaceuticals by the Ammonia-Oxidizing Archaeon *Nitrososphaera gargensis*. Environ.  
428 Sci. Technol. 50, 4682-4692.

- 429 Miao, X.-S., Metcalfe, C.D., 2003. Determination of carbamazepine and Its metabolites in  
430 aqueous samples using liquid chromatography–electrospray tandem mass spectrometry.  
431 Anal. Chem. 75, 3731-3738.
- 432 Pérez, S., Eichhorn, P., Celiz, M.D., Aga, D.S., 2006. Structural characterization of metabolites  
433 of the X-ray contrast agent iopromide in activated sludge using ion trap mass spectrometry.  
434 Anal. Chem. 78, 1866-1874.
- 435 Pomiès, M., Choubert, J.M., Wisniewski, C., Miège, C., Budzinski, H. Coquery, M., 2015. Lab-  
436 scale experimental strategy for determining micropollutant partition coefficient and  
437 biodegradation constants in activated sludge. Environ. Sci. Pollut. Res. 22, 4383-4395.
- 438 Prasse, C., Schlüsener, M.P., Schulz, R., Ternes, T.A., 2010. Antiviral drugs in wastewater and  
439 surface waters: a new pharmaceutical class of environmental relevance? Environ. Sci.  
440 Technol. 44, 1728-1735.
- 441 Prasse, C., Wagner, M., Schulz, R., Ternes, T.A., 2011. Biotransformation of the antiviral drugs  
442 acyclovir and penciclovir in activated sludge treatment. Environ. Sci. Technol. 45, 2761-  
443 2769.
- 444 Quintana, J.B., Weiss, S., Reemtsma, T., 2005. Pathways and metabolites of microbial  
445 degradation of selected acidic pharmaceutical and their occurrence in municipal wastewater  
446 treated by a membrane bioreactor. Water Res. 39, 2654-2664.
- 447 Radniecki, T.S., Dolan, M.E. Semprini, L., 2008. Physiological and transcriptional responses of  
448 *Nitrosomonas europaea* to toluene and benzene inhibition. Environ. Sci. Technol. 42, 4093-  
449 4098.

- 450 Rasche, M.E., Hicks, R.E., Hyman, M.R., Arp, D.J., 1990. Oxidation of monohalogenated  
451 ethanes and n-chlorinated alkanes by whole cells of *Nitrosomonas europaea*. J. Bacteriol.  
452 172, 5368-5373.
- 453 Rattier, M., Reungoat, J., Keller, J. Gernjak, W., 2014. Removal of micropollutants during  
454 tertiary wastewater treatment by biofiltration: Role of nitrifiers and removal mechanisms.  
455 Water Res. 54, 89-99.
- 456 Sathyamoorthy, S., Chandran, K. Ramsburg, C.A., 2013. Biodegradation and cometabolic  
457 modeling of selected beta blockers during ammonia oxidation. Environ. Sci. Technol. 47,  
458 12835-12843.
- 459 Sirés, I., Brillas, E., 2012. Remediation of water pollution caused by pharmaceutical residues  
460 based on electrochemical separation and degradation technologies: A review. Environ. Int.  
461 40, 212-229.
- 462 Skotnicka-Pitak, J., Khunjar, W.O., Love, N.G., Aga, D.S., 2009. Characterization of metabolites  
463 formed during the biotransformation of 17 $\alpha$ -ethinylestradiol by *Nitrosomonas europaea* in  
464 batch and continuous flow bioreactors. Environ. Sci. Technol. 43, 3549-3555.
- 465 Ternes, T.A., 1998. Occurrence of drugs in German sewage treatment plants and rivers. Water  
466 Res. 32, 3245-3260.
- 467 Ternes, T.A., Bonerz, M., Herrmann, N., Teiser, B., Andersen, H.R., 2007. Irrigation of treated  
468 wastewater in Braunschweig, Germany: An option to remove pharmaceuticals and musk  
469 fragrances. Chemosphere 66, 894-904.
- 470 Tijani, J.O., Fatoba, O.O., Petrik, L.F., 2013. A review of pharmaceuticals and endocrine-  
471 disrupting compounds: Sources, effects, removal, and detections. Water, Air, Soil Pollut.  
472 224, 1770-1798.

- 473 Tran, N.H., Urase, T., Ngo, H.H., Hu, J., Ong, S.L., 2013. Insight into metabolic and  
474 cometabolic activities of autotrophic and heterotrophic microorganisms in the  
475 biodegradation of emerging trace organic contaminants. *Bioresour. Technol.* 146, 721-731.
- 476 Xu, Y., Yuan, Z. Ni, B.-J., 2016. Biotransformation of pharmaceuticals by ammonia oxidizing  
477 bacteria in wastewater treatment processes. *Sci. Total Environ.* 566–567, 796-805.
- 478 Yi, T. Harper Jr, W.F., 2007. The link between nitrification and biotransformation of 17 $\alpha$ -  
479 ethinylestradiol. *Environ. Sci. Technol.* 41, 4311-4316.

480

**Table and figure legends**

481

482 **Table 1.** Conditions of conducted batch experiments with acyclovir (same design of key  
483 experimental conditions for experiments at initial acyclovir of  $15 \text{ mg L}^{-1}$  and  $15 \text{ } \mu\text{g L}^{-1}$ )

484

485 **Table 2.** The acyclovir removal efficiency, biotransformation efficiency and degradation  
486 constant in the conducted biodegradation experiments (high, initial acyclovir concentration of  $15$   
487  $\text{mg L}^{-1}$ ; low, initial acyclovir concentration of  $15 \text{ } \mu\text{g L}^{-1}$ ) with possible mechanisms involved

488

489 **Figure 1.** Concentration profiles of acyclovir and its product normalized to the initial acyclovir  
490 of (A)  $15 \text{ mg L}^{-1}$  and (B)  $15 \text{ } \mu\text{g L}^{-1}$  in the experiments with ammonia oxidation.

491

492 **Figure 2.** (A) Ammonia oxidation rate during the time course in the acyclovir biodegradation  
493 experiments with ammonia oxidation; (B) the relationship between acyclovir degradation rate  
494 and ammonia oxidation rate in the presence of ammonium.

495

496 **Figure 3.** Concentration profiles of acyclovir and its product normalized to the initial (A)  $15 \text{ mg}$   
497  $\text{L}^{-1}$  and (B)  $15 \text{ } \mu\text{g L}^{-1}$  in the experiments without ammonia addition.

498

499 **Figure 4.** Concentration profiles of acyclovir and its product normalized to the initial (A)  $15 \text{ mg}$   
500  $\text{L}^{-1}$  and (B)  $15 \text{ } \mu\text{g L}^{-1}$  in the experiments with inhibition of ammonia oxidation of AOB by  
501 allythiourea (ATU) addition.

502

503 **Figure 5.** The fragmentation pathways of P239 under ESI+ conditions derived from  $\text{MS}^2$   
504 experiments in the QqLIT mass spectrometer.

505



506 **Table 1.** Conditions of conducted batch experiments with acyclovir (same design of key  
 507 experimental conditions for experiments at initial acyclovir of 15 mg L<sup>-1</sup> and 15 µg L<sup>-1</sup>)

Experiments	EXP1	EXP2	EXP3	EXP4	EXP5
Initial ammonium (mg L <sup>-1</sup> )	50	0	50	50	50
Ammonium control	Constant	0	Constant	Constant	Constant
Approximate VSS (mg L <sup>-1</sup> )	1000	1000	1000	1000	0
Volume (L)	4	4	4	4	4
ATU (mg L <sup>-1</sup> )	0	0	30	0	0
NaN <sub>3</sub> (mg L <sup>-1</sup> )	0	0	0	500	0

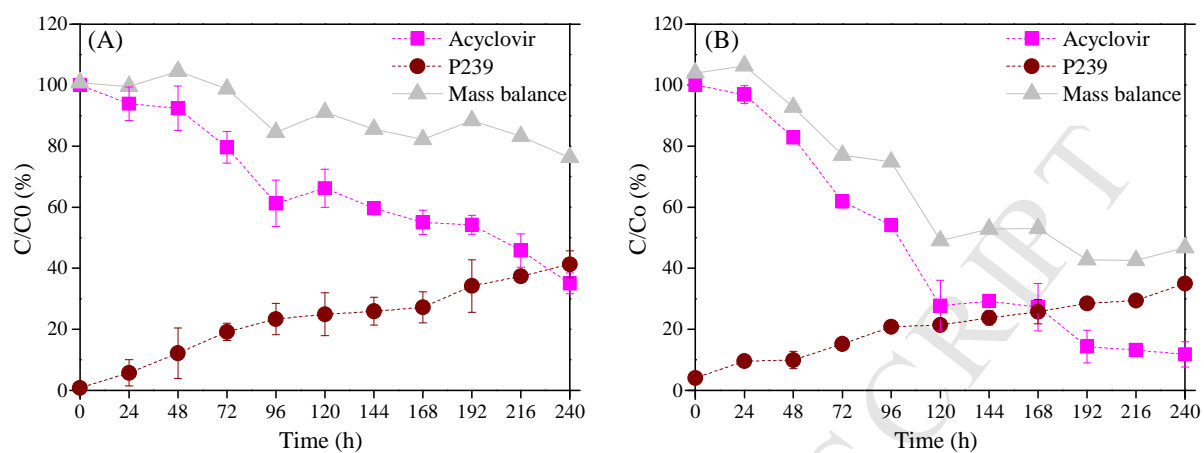
508 **Table 2.** The acyclovir removal efficiency, biotransformation efficiency and degradation  
 509 constant in the conducted biodegradation experiments (high, initial acyclovir concentration of 15  
 510 mg L<sup>-1</sup>; low, initial acyclovir concentration of 15 µg L<sup>-1</sup>) with possible mechanisms involved

Experiments	EXP1-high	EXP1-low	EXP2-high	EXP2-low	EXP3-high	EXP3-low
Removal efficiency (%)	65.1	88.2	40.9	47.8	36.2	50.3
Biotransformation efficiency (%)	58.6	33.0	~100	72.6	94.1	83.8
Biodegradation constant	0.0034 L gvss <sup>-1</sup> h <sup>-1</sup>	0.0071 L gvss <sup>-1</sup> h <sup>-1</sup>	0.027 mg gvss <sup>-1</sup> h <sup>-1</sup>	0.043 µg gvss <sup>-1</sup> h <sup>-1</sup>	0.02 mg gvss <sup>-1</sup> h <sup>-1</sup>	0.018 µg gvss <sup>-1</sup> h <sup>-1</sup>
Main mechanisms	Cometabolism by AOB		Metabolism by AOB and heterotrophs		Metabolism by heterotrophs	

511

512

513

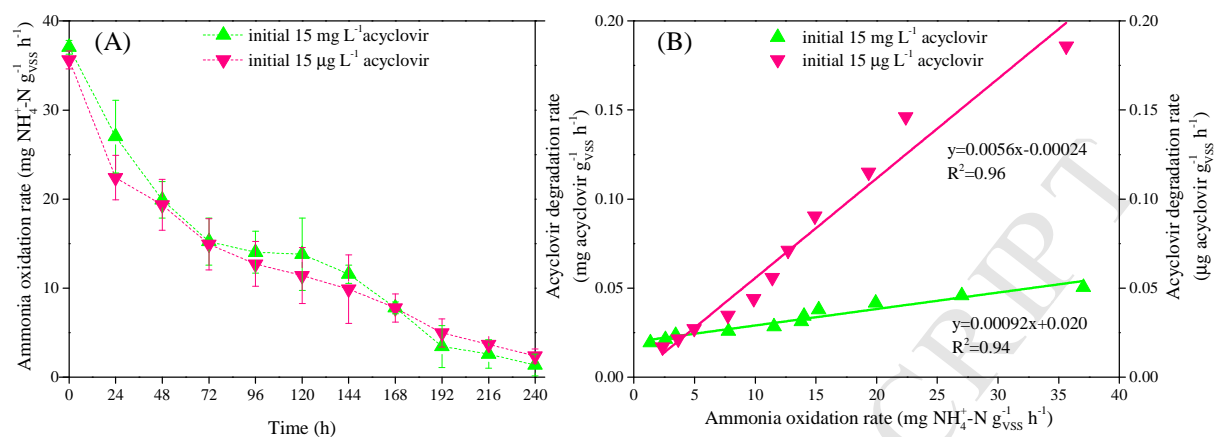


514

515 **Figure 1.** Concentration profiles of acyclovir and its product normalized to the initial acyclovir  
516 of (A) 15 mg L<sup>-1</sup> and (B) 15 µg L<sup>-1</sup> in the experiments with ammonia oxidation.

517

518

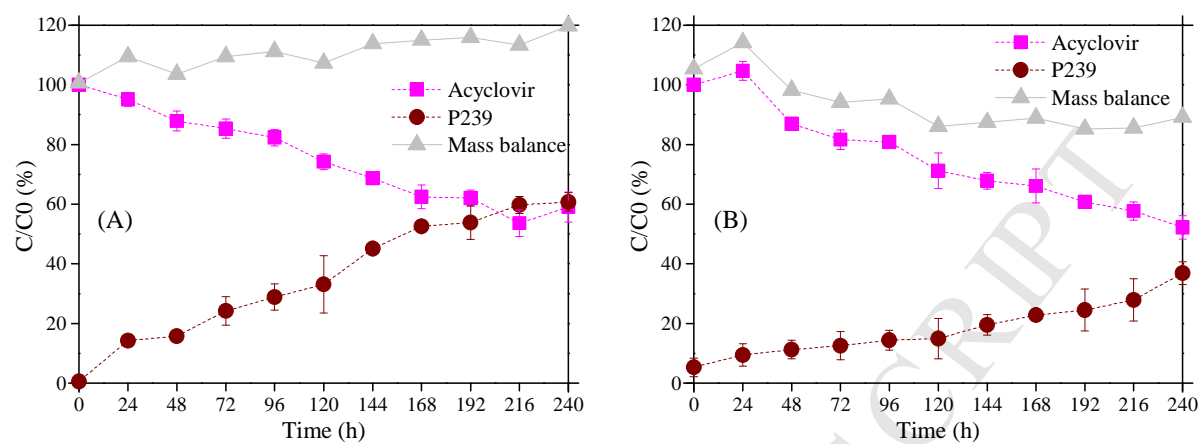


519

520 **Figure 2.** (A) Ammonia oxidation rate during the time course in the acyclovir biodegradation  
 521 experiments with ammonia oxidation; (B) the relationship between acyclovir degradation rate  
 522 and ammonia oxidation rate in the presence of ammonium.

523

524



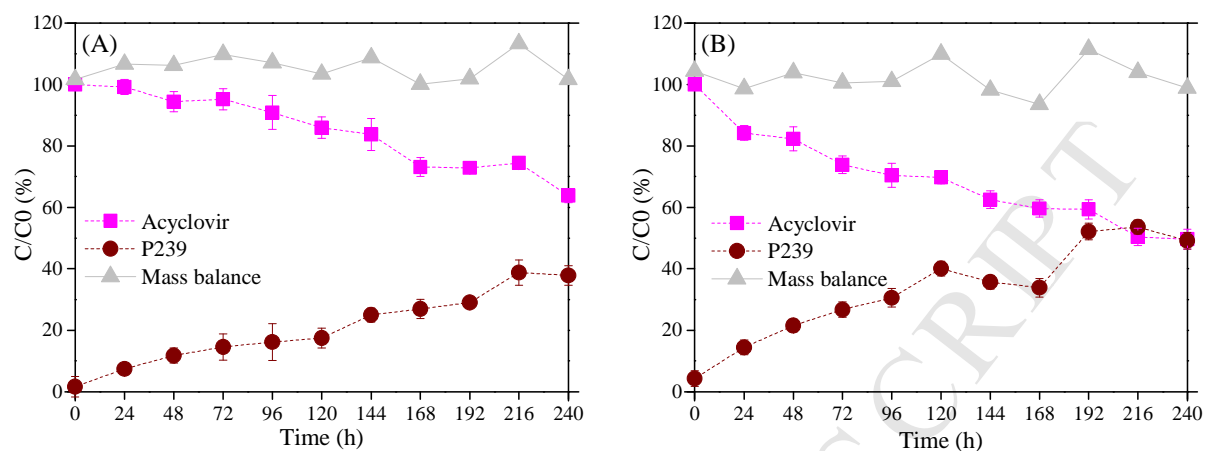
525

526

527 **Figure 3.** Concentration profiles of acyclovir and its product normalized to the initial (A) 15 mg528 L<sup>-1</sup> and (B) 15 μg L<sup>-1</sup> in the experiments without ammonia addition.

529

530



531

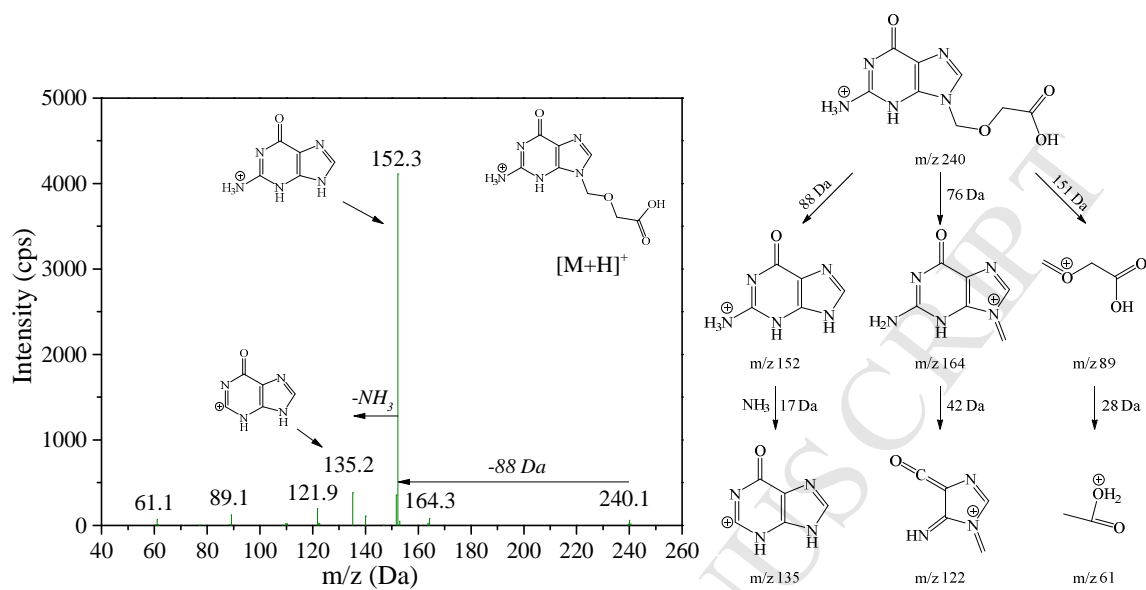
532

533 **Figure 4.** Concentration profiles of acyclovir and its product normalized to the initial (A) 15 mg534 L<sup>-1</sup> and (B) 15 µg L<sup>-1</sup> in the experiments with inhibition of ammonia oxidation of AOB by

535 allythiourea (ATU) addition.

536

537



538

539

540 **Figure 5.** The fragmentation pathways of P239 under ESI<sup>+</sup> conditions derived from MS<sup>2</sup>

541 experiments in the QqLIT mass spectrometer.

**Highlights**

- Acyclovir biodegradation followed cometabolism by AOB in the presence of ammonium.
- Alcohol oxidation was the main biotransformation pathway producing carboxy-acyclovir.
- Formation of carboxy-acyclovir was independent on the initial concentration of acyclovir.
- Metabolic type has no effect on the biotransformation pathway into carboxy-acyclovir.
- The enzyme-linked oxidation could be catalyzed by AOB or heterotrophs.